Journal of Engineering Physics and Thermophysics, Vol. 72, No. 3, 1999

NUMERICAL MODELING OF DROPLET DEPOSITION IN CHANNELS OF INTRICATE SHAPE

É. F. Shurgal'skii and I. Kh. Enikeev

UDC 532.529

Numerical modeling of two-phase flows in channels of intricate configuration is conducted. Problems of the stability of the proposed algorithm for highly subsonic flows are studied. The effect of various physicomechanical parameters on the flow structure in corrugated channels is considered.

Introduction. Gas-droplet flows are widely used in atomic-power engineering, chemical engineering, and other technological areas for enhancing the processes of heat and mass transfer and separation. Optimum design of inertial, centrifugal, and vortex separators and calculation of the process modes in them require information on the hydrodynamic parameters of the flow. Therefore, equations of interpenetrating continua with appropriate assumptions [1] were used as a mathematical model describing gas-droplet flow in these devices. Relying on the method of large particles, we propose an algorithm for calculating the parameters of a two-phase (in the general case the medium can be multiphase) medium that is based on conversion to new independent variables (x, ξ). This technique permits conformal mapping of a region in the physical plane of intricate configuration onto a region in the computational plane in a shape of a square as a rectangle.

1. Mathematical Model of Two-Phase Flow in the Variables (x, ξ). Let us consider a highly subsonic flow of a two-phase medium consisting of a compressible carrier gas and monodisperse droplets, in louvers of finite length L (see Fig. 1). We present, in dimensionless form, equations and closing relations that describe an unsteady two-dimensional flow of a monodisperse two-phase medium within the framework of the model of interpenetrating continua:

$$\frac{\partial \rho_s}{\partial t} + \nabla^k (\rho_s v_s^k) = 0 \quad (s = 1, 2),$$

$$\frac{\partial \rho_s \vec{v_s}}{\partial t} + \nabla^k (\rho_s v_s^k \vec{v_s}) = -\frac{\delta}{\alpha} \vec{\nabla} p + F,$$

$$\sum_{s=1}^{2} \left\{ \frac{\partial \rho_s E_s}{\partial t} + \nabla^k [(\rho_s E_s + \delta p/\alpha) v_s^k] \right\} = 0, \tag{1}$$

$$\frac{\partial \rho_2 e_2}{\partial t} + \nabla^k (\rho_2 e_2 v_2^k) = q, \quad q = \pi n d \lambda (T_1 - T_2),$$

$$E_s = e_s + \frac{1}{2} (\vec{v_s}, \vec{v_s}), \quad \alpha = \gamma M_0^2, \quad \delta = \begin{cases} 1, s = 1 \\ 0, s = 2 \end{cases}.$$

System (1) should be completed with the equations of state of the phases, and here we assume that the carrying medium is an ideal gas and the droplets are incompressible (the true density of the droplets is $\rho_2^0 = 1000$ kg/m^3), and

$$p = (\gamma - 1) \rho e_1, \quad e_1 = c_{v1} T_1, \quad e_2 = c_2 T_2. \tag{2}$$

Moscow State Academy of Chemical Engineering, Russia. Translated from Inzhenerno-Fizicheskii Zhurnal, Vol. 72, No. 3, pp. 473-481, May-June, 1999. Original article submitted October 8, 1997.

1062-0125/99/7203-0445$22.00

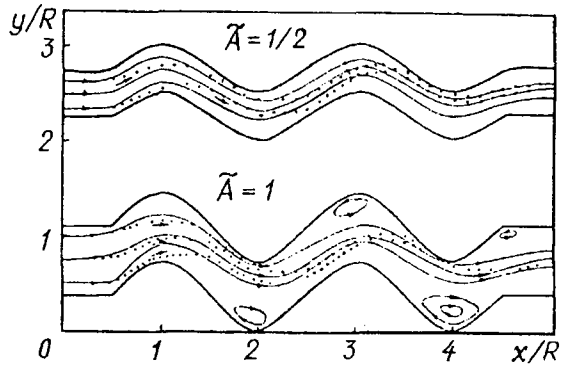

Fig. 1. Structure of a gas-droplet flow in corrugated channels (louvers) (m_{20} = 0.001, d = 8 μm). Light solid lines indicate the gas, dots the droplets, and heavy solid lines the a channel contour.

Dimensionless parameters in Eqs. (1) and (2) are introduced by the relations

$$\bar{v}_s = \frac{v_s}{V}, \quad \bar{p} = \frac{p}{p_0}, \quad \bar{\rho} = \frac{\rho}{\rho_0}, \quad \bar{e}_s = \frac{e}{e_0}, \quad \bar{E} = \frac{E}{E_0},$$

$$\bar{x} = \frac{x}{R}, \quad \bar{y} = \frac{y}{R}, \quad \bar{t} = \frac{t}{\tau} \tag{3}$$

(τ is the characteristic time in which a droplet travels the distance R with the characteristic velocity V).

For the vector of the friction force between the phases and the rate of interphasic heat transfer q we write the expressions

$$\vec{F} = \mathrm{Stk} \cdot \rho_2 (\vec{v}_1 - \vec{v}_2), \quad \mathrm{Stk} = \frac{\overset{0}{\rho_2} V d^2}{18 \mu R},$$

$$q = \beta^{(\tau)} \rho_2 \left(e_1 - e_2 \frac{c_{v1}}{c_2} \right), \quad \beta^{(\tau)} = \frac{\overset{0}{\rho_2} V d^2 c_{v1}}{12 \lambda_1 R}. \tag{4}$$

It should be noted that two-phase flows with monodisperse droplets or particles are really not observed, since in a disperse medium there is always a droplet (particle) size distribution usually specified in the form of a distribution function $f(r)$, for which use is most frequently made of the lognormal distribution law

$$f(r) = \frac{1}{\sqrt{2} \ln \sigma} \exp \left[- \left(\frac{\ln (r/r_0)}{\sqrt{2} \ln \sigma} \right)^2 \right],$$

where $r = d/2$, r_0 is the mathematical expectation, and $\ln \sigma$ is the rms deviation of the logarithms of the particle radii. Still, in some cases, for example, with bubbling of vapor through a liquid layer, the rms deviation of the sizes of the droplets carried out to the separation zone of a nuclear electric power plant is not greater than 8–10% of a some mean value r under certain conditions [2], and a monodisperse model of a two-phase continuum describes the flow of a read polydisperse medium to sufficient accuracy. Upon entering the gas flow, the liquid droplets deform, and for certain relationships between the forces of surface tension, viscosity, and inertia of the droplets they can break up into smaller ones. Because the splitting of the disperse inclusions fundamentally affects the interphase exchange in two-phase media, in the general case it should be accounted for by introducing appropriate source terms into the right-hand sides of Eqs. (1).

The study [1] showed that for this class of flows the splitting commences when the following condition is fulfilled:

$$\mathrm{We}_{12} \geq 0.5\,\mathrm{Re}_{12}^{0.5},$$

where $\mathrm{We}_{12} = \rho_1 d|\bar{v}_1 - \bar{v}_2|^2/\Sigma$, $\mathrm{Re}_{12} = \rho_1 d|\bar{v}_1 - \bar{v}_2|/\mu$, and $\Sigma = 73\cdot 10^{-3}$ kg/sec^{-2}.

In calculations the maximum droplet diameter was taken to be 100 μm, the flow velocity $v \sim 10$ m/sec, and therefore, $W_{\max} \sim 10^{-4}\cdot 10^2/10^{-1}$, and $\mathrm{Re}_{12} \sim 10^{-4}\cdot 10/10^{-5} \cong 100$. Hence, $\mathrm{We}_{12} << 0.5\mathrm{Re}_{12}^{0.5}$, and therefore in this problem droplet splitting can be disregarded.

To integrate Eqs. (1) and (2), boundary and initial conditions must be specified. On the left boundary of the region from which the gas-droplet flow issues, in the cross section $x = 0$ (see Fig. 1), we assigned the condition of constant flow velocity, i.e.,

$$V = 0,$$

and the conditions $H_0 = 0$ and $S = 0$ (H_0 and S are the total enthalpy and entropy of the mixture). Also, the reduced density and velocity of the phase on this section of the channel were assumed to be preset.

On the lateral walls, a nonleakage condition is fulfilled for the gas and an attachment condition is fulfilled for the droplets, i.e., the droplets that reached the channel walls vanish from the flow. At the channel outlet, the condition of pressure constancy in the surrounding space was used for the flow. Analyzing the results of numerous calculations revealed that the specific form of the boundary condition at the channel outlet (pressure constancy in the surrounding space, determination of the pressure from the Bernoulli equation, etc.) does not have a fundamental effect on the channel flow.

The parameters of the undisturbed flow $\vec{F} = 0$ and $q = 0$ in the cross section $X = 0$ were used as the initial data. Integration of system of equations (1) using a finite-difference method in the curvilinear region

$$Q\left\{0 \leq x \leq L/R,\ G(x) \leq y \leq F(x)\right\}$$

($G(x)$ and $F(x)$ are the equations of the lower and upper surfaces of the louvers) involves the need to replace the continuous region Q by a grid region, which, however, gives rise to irregular nodes (or calculation cells) near the region boundary. Therefore, it is reasonable to introduce new variables $\xi = \xi(x, y)$ and $\eta = \eta(x, y)$ in which the curvilinear region becomes rectangular. The studies [3, 4] showed that if in this case the Jacobian of the transformation $I = D(\xi, \eta)/D(x, y)$ exists and does not vanish at any point of the region, the divergent form of Eqs. (1) is retained. Upon substitution of the independent variable $\xi = [y - G(x)]/[F(x) - G(x)]$ the curvilinear region Q converts to the rectangular region N ($0 \leq x \leq 1$, $0 \leq \xi \leq 1$). Then, in the variables (x, ξ) system of Eqs. (1) takes the form

$$\frac{\partial \rho}{\partial t} + \frac{\partial \rho_s v_s^x}{\partial x} + \frac{\partial \rho_s U_s}{\varepsilon \partial \xi} = -\frac{\rho_s U_s^\varepsilon}{\varepsilon \xi},$$

$$\frac{\partial \rho_s v_s^x}{\partial t} + \frac{\partial \rho_s (v_s^x)^2}{\partial x} + \frac{\partial \rho_s v_s U_s}{\varepsilon \partial \xi} = \frac{1}{\alpha\varepsilon}\left[-\varepsilon \frac{\partial p}{\partial x} + (G' + \xi\varepsilon')\frac{\partial p}{\partial \xi}\right] - \frac{\rho_s v_s^x U_s^\varepsilon}{\varepsilon \xi} + (-1)^s F^x,$$

$$\frac{\partial \rho_s v_s^y}{\partial t} + \frac{\partial \rho_s v_s^y v_s^x}{\partial x} + \frac{\partial \rho_s v_s^y U_s}{\varepsilon \partial \xi} = -\frac{1}{\alpha \xi}\frac{\partial p}{\partial \xi} - \frac{\rho_s v_s^y U_s^\varepsilon}{\varepsilon \xi} + (-1)^s F^\xi, \tag{5}$$

$$\sum_{s=1}^{2}\left[\frac{\partial \rho_s E_s}{\partial t} + \frac{\partial\left(\rho_s E_s + \frac{\delta}{\alpha} p\right) v_s^x}{\partial x} + \frac{\partial\left(\rho_s E_s + \frac{\delta}{\alpha} p\right) U_s}{\varepsilon \partial \xi}\right] = 0,$$

$$\frac{\partial \rho_s e_2}{\partial t} + \frac{\partial \rho_2 e_2 v_2^x}{\partial x} + \frac{\partial \rho_2 e_2 U_2}{\varepsilon \partial \xi} = q - \frac{\rho_2 e_2 U_2^\varepsilon}{\varepsilon \xi},$$

$$\varepsilon(x) = F(x) - G(x), \quad U_s = v_s^y - v_s^x (G' + \xi\varepsilon'),$$

$$U_s^{\varepsilon} = \begin{cases} v_s^y + v_s^x (G' + \xi\varepsilon') & - \text{ for an axisymmetric flow}, \\ v_s^x (G' + \xi\varepsilon') & - \text{ for a plane flow}. \end{cases}$$

2. Eulerian Step of the Method of Large Particles for $M_0 << 1$. We present the equations describing the gas flow at the Eulerian step in the following form:

$$\frac{\partial u}{\partial t} = -\frac{1}{\alpha\rho}\frac{\partial p}{\partial x} + \frac{(G' + \xi\varepsilon')}{\varepsilon\alpha\rho}\frac{\partial p}{\partial \xi},$$

$$\frac{\partial v}{\partial t} = -\frac{1}{\alpha\varepsilon\rho}\frac{\partial p}{\partial \xi}, \tag{6}$$

$$\frac{\partial p}{\partial t} = -\frac{(\gamma - 1)}{\varepsilon} p \left[\frac{\partial \varepsilon u}{\partial x} + \frac{\partial (v - \xi\varepsilon' u)}{\partial \xi}\right].$$

In system (6), the terms that take account of the axial symmetry, convective transfer, and interphase interaction are disregarded. The considered integration region is covered with a fixed calculation grid with rectangular cells of sides Δx and $\Delta\xi$. We now write system of equations (6) in difference form by the following implicit scheme:

$$u_{i,j}^{n+1} = u_{i,j}^{n} - \frac{\chi}{\alpha\rho_{i,j}^{n}}(p_{i+1/2,j}^{n+1} - p_{i-1/2,j}^{n+}) + \frac{(G_i' + \varepsilon_i'\xi_j)}{\varepsilon_i \alpha \rho_{i,j}^{n}}(p_{i,j+1/2}^{n+1} - p_{i,j-1/2}^{n+1}), \tag{7}$$

$$v_{i,j}^{n+1} = v_{i,j}^{n} - \frac{\chi}{\alpha\,\varepsilon_i \rho_{i,j}^{n}}(p_{i,j+1/2}^{n+1} - p_{i,j-1/2}^{n+1}), \tag{8}$$

$$p_{i,j}^{n+1} = p_{i,j}^{n} - \frac{(\gamma - 1)\chi p_{i,j}^{n+1}}{\varepsilon_i}[\varepsilon_i (u_{i+1/2,j}^{n+1} - u_{i-1/2,j}^{n+1}) + v_{i,j+1/2}^{n+1} - v_{i,j-1/2}^{n+1} -$$

$$- (\varepsilon_i' \xi_{j+1/2} + G_i') u_{i,j+1/2}^{n+1} + (\varepsilon_i' \xi_{j-1/2} + G_i') u_{i,j-1/2}^{n+1}], \tag{9}$$

where $\chi = \Delta t/\Delta x$.

With the aid of Eqs. (8)-(9) we eliminate the quatities of $u_{i,j}^{n+1}$ and $v_{i,j}^{n+1}$ in the $(n+1)$-th time step from Eq. (7). We introduce the notation

$$A_i = \frac{\chi^2 (\gamma - 1) p_{i,j}^{n+1}}{\alpha\varepsilon_i}\left[\frac{\varepsilon_i}{\rho_{i-1/2,j}^{n}} + \frac{1}{4}\left(\frac{\varepsilon_i' \xi_{j+1/2} + G_i'}{\rho_{i,j+1/2}^{n}} + \frac{\varepsilon_i' \xi_{j-1/2} + G_i'}{\rho_{i,j-1/2}^{n}}\right)\right],$$

$$B_i = \frac{\chi^2 (\gamma - 1) p_{i,j}^{n+1}}{\alpha\varepsilon_i}\left[\frac{\varepsilon_i}{\rho_{i+1/2,j}^{n}} - \frac{1}{4}\left(\frac{\varepsilon_i' \xi_{j+1/2} + G_i'}{\rho_{i,j+1/2}^{n}} - \frac{\varepsilon_i' \xi_{j-1/2} + G_i'}{\rho_{i,j-1/2}^{n}}\right)\right],$$

$$C_i = 1 + A_i + B_i + \frac{\chi^2 (\gamma - 1) p_{i,j}^{n+1}}{\alpha\varepsilon^2}\left(\frac{1 + (\varepsilon_i')^2 \xi_{j+1/2}^2}{\rho_{i,j+1/2}^{n}} + \frac{1 + (\varepsilon_i')^2 \xi_{j-1/2}}{\rho_{i,j-1/2}^{n}}\right),$$

$$A_j^* = \frac{\chi^2 (\gamma - 1)\, p_{i,j}^{n+1}}{\alpha \varepsilon_i} \left[\frac{1 + (\varepsilon_i')^2 \xi_{j+1/2}^2}{\varepsilon_i \overset{n}{\rho}_{i,j+1/2}} - \frac{(G_i' + \varepsilon_i' \xi_j)}{4} \left(\frac{\varepsilon'_{i+1/2}}{\varepsilon_{i+1/2} \overset{n}{\rho}_{i+1/2,j}} - \frac{\varepsilon'_{i-1/2}}{\varepsilon_{i-1/2} \overset{n}{\rho}_{i+1/2,j}} \right) \right],$$

$$B_j^* = \frac{\chi^2 (\gamma - 1)\, p_{i,j}^{n+1}}{\alpha \varepsilon_i} \left[\frac{1 + (\varepsilon_i')^2 \xi_{j+1/2}^2}{\varepsilon_i \overset{n}{\rho}_{j-1/2}} + \frac{(G_i' + \varepsilon_i' \xi_j)}{4} \left(\frac{\varepsilon'_{i+1/2}}{\varepsilon_{i+1/2} \overset{n}{\rho}_{i+1/2,j}} - \frac{\varepsilon'_{i-1/2}}{\varepsilon_{i-1/2} \overset{n}{\rho}_{i-1/2,j}} \right) \right],$$

$$\Phi_i^* = - p_{i,j}^n - A_j^* p_{i,j-1}^{n+1} - B_j^* p_{i,j+1}^{n+1} + \frac{\chi^2 (\gamma - 1)\, p_{i,j}^{n+1}}{4 \alpha \varepsilon_i} [(p_{i+1,j+1}^{n+1} -$$

$$- p_{i+1,j-1}^{n+1}) \frac{\varepsilon_i (\varepsilon'_{i+1/2} \xi_j + G'_{i+1/2})}{\varepsilon_{i+1/2} \overset{n}{\rho}_{i+1/2,j}} + (p_{i+1,j+1}^{n+1} - p_{i-1,j-1}^{n+1}) \left(\frac{\varepsilon_i' \xi_{i+1/2} + G_i'}{\overset{n}{\rho}_{i,j-1/2}} \right) -$$

$$- (p_{i-1,j+1}^{n+1} - p_{i-1,j-1}^{n+1}) \frac{\varepsilon_i (\varepsilon'_{i-1/2} \xi_i - G'_{i-1/2})}{\varepsilon_{i-1/2} \overset{n}{\rho}_{i-1/2,j}} - (p_{i+1,j-1}^{n+1} - p_{i-1,j-1}^{n+1}) \frac{\varepsilon_i' \xi_{j-1/2} + G_i'}{\overset{n}{\rho}_{i,j-1/2}} \Bigg].$$

Then, Eq. (7) is written as

$$A_i p_{i-1,j}^{n+1} - C_i p_{i,j}^{n+1} + B_i p_{i+1,j}^{n+1} = \Phi_i \tag{10}$$

for longitudinal factorization and as

$$A_j^* p_{i,j-1}^{n+1} - C_j^* p_{i,j}^{n+1} + B_j^* p_{i,j+1}^{n+1} = \Phi_j^*, \quad C_j^* = C_i, \quad \Phi_j^* = \Phi_i \tag{11}$$

for transverse factorization. Since the factorization coefficients in Eqs. (10) and (11) are functions of $p_{i,j}^{n+1}$, the latter were solved using an iteration with respect to $p_{i,j}^{n+1}$.

In each iteration, the values of the quantities p_{ij}^{n+1} entering into the expressions for A_i, B_i, A_j^*, B_j^*, C_i, C_j^*, Φ_i, and Φ_j^* were replaced by the corresponding values taken from the preceding iteration. After solving system (7)-(9) to the prescribed accuracy the pressure and velocities of the carrying phase are determined in the Eulerian step. All parameters of the disperse phase in the Eulerian step do not vary with time.

The Lagrangian and final steps are carried out in accordance with the general scheme of the method of large particles [5].

3. Stability Analysis of the Modified Method of Large Particles in the Variables (x, ξ). We consider the problem of the stability of the proposed difference scheme. We will use results [5, 6] based on an analysis of the parabolic form of the first differential approximation of the scheme.

Since there is no itrinsic pressure in the particle medium, the equations of motion of the disperse phase are integrated by an explicit scheme of the method of large particles [5]. The scheme is well-known in the literature, and therefore the pertinent equations in the initial system of equations (1) are not considered in this section. Since the terms that take into account the intensity of the interphase force and thermal interaction, generally speaking, do not have any effect on the stability of the numerical scheme, the equations of the final step for the gas phase are taken without regard for the forces of interphase interaction. Without limiting the generality of the investigation we suppose that the flow is plane. Thus, with a view to the above remarks the equations of the final step for the gas have the form

$$\rho_{i,j}^{n+1} = \rho_{i,j}^n + \frac{1}{2} \frac{\Delta t}{\Delta x} \Big\{ \rho_{i-1,j}^n (\tilde{u}_{i-1,j} + \tilde{u}_{i,j}) - \rho_{i,j}^n (\tilde{u}_{i,j} + \tilde{u}_{i,j}) +$$

$$+ \frac{1}{3} [\rho_{i,j-1}^n (\tilde{U}_{i,j-1} + \tilde{U}_{i,j}) - \rho_{i,j}^n (\tilde{U}_{i,j} + \tilde{U}_{i,j+1})] \Big\} - \rho_{i,j}^n \tilde{U}_{i,j}^{\varepsilon},$$

$$\rho_{i,j}^{n+1}\, u_{i,j}^{n+1} = \rho_{i,j}^{n}\, \tilde{u}_{i,j} + \frac{\Delta t}{2\Delta x}\left\{\rho_{i-1,j}^{n}\, \tilde{u}_{i-1,j}\,(\tilde{u}_{i-1,j} + \tilde{u}_{i,j}) - \right.$$

$$- \rho_{i,j}^{n}\,(\tilde{u}_{i,j} + \tilde{u}_{i+1,j})\,\tilde{u}_{i,j} + \frac{1}{\varepsilon_i}\,[\rho_{i,j-1}^{n}\,\tilde{u}_{i,j-1}\,(\tilde{U}_{i,j-1} + \tilde{U}_{i,j}) -$$

$$\left. - \rho_{i,j}^{n}\,\tilde{u}_{i,j}\,(\tilde{U}_{i,j} + \tilde{U}_{i,j+1})\,]\right\} - \rho_{i,j}\,\tilde{u}_{i,j}\,\tilde{U}_{i,j}^{\varepsilon}\,\Delta t\,,$$

$$\rho_{i,j}^{n+1}\, v_{i,j}^{n+1} = \rho_{i,j}^{n}\, \tilde{v}_{i,j} + \frac{\Delta t}{2\Delta x}\left\{(\rho_{i-1,j}^{n}\, \tilde{v}_{i-1,j}\,(\tilde{u}_{i-1,j} + \tilde{u}_{i,j}) - \right.$$

$$- \rho_{i,j}^{n}\,\tilde{v}_{i,j}\,(\tilde{u}_{i,j} + \tilde{u}_{i+1,j}) + \frac{1}{\varepsilon_i}\,[\rho_{i,j-1}^{n}\,\tilde{v}_{i,j-1}\,(\tilde{U}_{i,j-1} + \tilde{U}_{i,j}) -$$

$$\left. - \rho_{i,j}^{n}\,\tilde{v}_{i,j}\,(\tilde{U}_{i,j} + \tilde{U}_{i,j+1})\,]\right\} - \rho_{i,j}\,\tilde{v}_{i,j}\,\tilde{U}_{i,j}^{\varepsilon}\,\Delta t\,, \qquad (12)$$

$$\rho_{i,j}^{n+1}\, E_{i,j}^{n+1} = \rho_{i,j}^{n}\, \tilde{E}_{i,j} + \frac{\Delta t}{2\Delta x}\left\{\rho_{i-1,j}^{n}\, \tilde{E}_{i-1,j}\,(\tilde{u}_{i-1,j} + \tilde{u}_{i,j}) - \right.$$

$$- \rho_{i,j}^{n}\,\tilde{E}_{i,j}\,(\tilde{u}_{i,j} + \tilde{u}_{i+1,j}) + \frac{1}{\varepsilon_i}\,[\rho_{i,j-1}^{n}\,\tilde{E}_{i,j-1}\,(\tilde{U}_{i,j-1} + \tilde{U}_{i,j}) -$$

$$\left. - \rho_{i,j}^{n}\,\tilde{E}_{i,j}\,(\tilde{U}_{i,j} + \tilde{U}_{i,j+1})\,]\right\} - \rho_{i,j}\,\tilde{E}_{i,j}\,\tilde{U}_{i,j}^{\varepsilon}\,\Delta t\,,\quad \tilde{U}_{i,j}^{\varepsilon} = \tilde{u}_{i,j}\varepsilon_i'/\varepsilon_i\,.$$

It was assumed here that $\tilde{u}_{i-1,j} + \tilde{u}_{i,j} > 0$, $\tilde{U}_{i,j-1} + \tilde{U}_{i,j} > 0$, etc. Analysis of the stability for cells in which the inequality sign is reversed is performed in a similar fashion. Substituting relations (7)-(9) for $\tilde{u}$, $\tilde{v}$, and $\tilde{p}$ into Eqs. (12) of the final step and representing the parabolic form of the first differential approximation of difference scheme (12) as

$$L(f) = A\,\frac{\partial^2 f}{\partial x^2} + B\,\frac{\partial^2 f}{\partial \xi^2} + C\,\frac{\partial^2 f}{\partial x \partial \xi} + \Delta_f\,,$$

we obtain expressions for the diagonal elements of the matrices A, B, and C

$$A_{11}^{\rho} = \frac{1}{2}\left\{u\Delta x + \Delta t\left[\frac{p\,(1 + \varepsilon^2 + (\varepsilon')^2\,\xi^2)}{\alpha\rho\varepsilon^2} - u^2\right]\right\},$$

$$B_{11}^{\rho} = \frac{1}{2}\left\{U_{\Delta x} + \frac{\Delta t}{\varepsilon}\left[\frac{\varepsilon'\,\xi\Delta x}{\alpha\rho}\,\frac{\partial \rho}{\partial x} + \frac{(1 + (\varepsilon')^2\,\xi^2)}{\alpha\rho}\,p - \frac{U^2}{\varepsilon}\right]\right\},$$

$$C_{11}^{\rho} = -\frac{1}{\varepsilon}\left(uU + \frac{\varepsilon'\xi p}{\alpha\rho}\right)\Delta t\,,$$

$$A_{22}^{u} = \frac{1}{2}\left\{\rho u\Delta x + \Delta t\left[\frac{\gamma p}{\rho} - \rho u^2\,(2\gamma^2 - 5\gamma - 6)\right]\right\},$$

$$B_{22}^{u} = \frac{1}{2\varepsilon}\left\{\rho U\Delta x + \frac{\Delta t}{\varepsilon}\left[\frac{\gamma p\,(\varepsilon')^2\,\xi^2}{\alpha} + [\varepsilon'\xi\,(U - 2u\varepsilon'\xi) - \right.\right.$$

$$\left.\left. - (\gamma - 1)\,(u\,(1 + (\varepsilon')^2\,\xi^2) - U\varepsilon'\xi)\,]\rho u\right]\right\}, \qquad (13)$$

$$C_{22}^{u} = \frac{\Delta t}{\varepsilon}\left\{-\frac{\varepsilon'\xi\gamma p}{\alpha} + \frac{\rho u}{2}\left[u\varepsilon'\xi\,(5-2\gamma) + U + \right.\right.$$

$$\left.\left. + (\gamma-1)\,(U-u) + (\gamma-1)\,(2\gamma-1)\,(U-\varepsilon'\xi u)\right]\right\},$$

$$A_{33}^{v} = \frac{1}{2}\left\{\rho u\Delta x - \Delta t\rho\left[u^2 + (\gamma-1)\,v^2\right]\right\},$$

$$B_{33}^{v} = \frac{1}{2}\left\{\rho U\Delta x - \frac{\Delta t}{\varepsilon^2}\left[\frac{\gamma p}{\alpha} - \rho v\left[\frac{U+2v}{2} + U\,(\gamma-1)\,(2\gamma-1)\right]\right]\right\},$$

$$C_{33}^{v} = -\frac{\Delta t\rho v}{\varepsilon}\left[2U + u\,(4-\gamma) + 3v\varepsilon'\xi\,(\gamma-1) + u\,(\gamma-1)\,(2\gamma-1)\right],$$

$$A_{44}^{E} = \rho\left\{\frac{u\Delta x}{2} + \Delta t\left[(\gamma-1)\,E + (\gamma^2+\gamma-1)\,u^2\right]\right\},$$

$$B_{44}^{E} = \frac{\rho}{\varepsilon}\left\{\frac{u\Delta x}{2} + \frac{\Delta t}{\varepsilon}\left[(\gamma^2+\gamma-1)\,U^2 + (1+(\varepsilon')^2\xi^2)\,E\right]\right\},$$

$$C_{44}^{E} = \frac{2\rho U u\gamma^2\Delta t}{\varepsilon}.$$

In expressions (13), the superscript of the coefficients on the left-hand sides indicates the variable to which the coefficient relates.

In conformity with results of [5], the stability criteria for the presented modification of the scheme of the method of large particles are conditions of positiveness for the diagonal elements of the matrices A and B. An important difference of the expressions for the coefficients A_{kk} and B_{kk} in Eqs. (13) from similar expressions for these coefficients obtained with an explicit scheme of the Eulerian step of the method of large particles lies in the following. Terms of the type p/α enter the right-hand sides of A_{kk} and B_{kk} with a "plus" sign in the case of an implicit scheme and with a "minus" sign in the case of an explicit scheme. At low subsonic velocities, when $\alpha \ll 1$, these terms make a major contribution to the value on the right-hand sides of the equations for A_{kk} and B_{kk}. This circumstance weakens significantly the constraints on the value of the ratios $\Delta t/\Delta x$ for $\alpha \ll 1$ that are stipulated by the requirement of stability of the difference scheme. When $\alpha \gg 1$, the contribution of terms of the type p/α becomes of the same order of magnitude as $\rho\bar{u}^2$. In this case the stability conditions for an implicit scheme become practically the same as for an explicit scheme, which renders the use of implicit schemes for large α unreasonable.

It should be noted that, for small α, terms of the type p/α make the right-hand sides of the coefficients A_{kk} and B_{kk} positive for any $\Delta t/\Delta x$. Nonetheless, as the authors of [4] showed, the presence of an iteration process in the integration of the equations in the Eulerian step leads to constraints on $\Delta t/\Delta x$. The practice of calculations shows that an implicit scheme is stable for $\Delta t/\Delta x = 0.1$ when $\alpha \geq 0.001$.

To analyze the accuracy of the results obtained we investigated the effect of the scheme viscosity on the flow structure in a channel by varying the number of cells of the calculation region per unit length. In all calculations the parameters differed by no more than 3–5%.

Below we present some results calculated using the devised technique for gas-droplet flows in corrugated channels for which the equations of the lower and upper boundaries had the form

$$Y_{\text{low}} = \begin{cases} 1/6, & 0 \leq x \leq 1/3 \\ 1/6, & [\sin\pi\,(3x-1)/2 + 1], \quad 1/3 \leq x \leq 1, \\ 1/6, & x > 1 \end{cases}$$

$$Y_{\text{up}} = Y_{\text{low}} + 1/3.$$

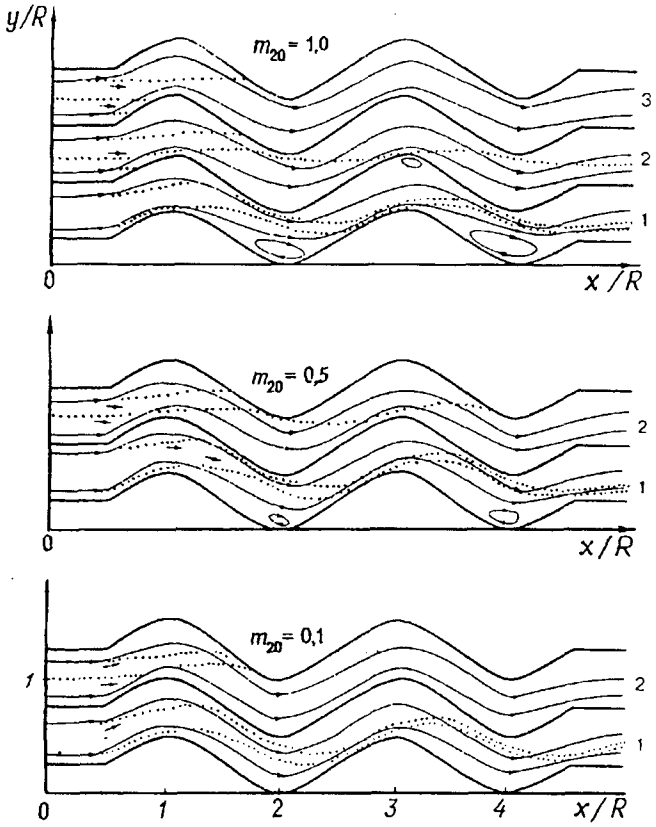

Fig. 2. Gas and droplet streamlines in louvers for various values of m_{20}, d: 1) $d = 10\ \mu$m, 2) 20, 3) 80.

As the carrier phase we considered air with $\rho_{10}^0 = 1.21$ kg/m^3 and $\mu_0 = 1.75 \cdot 10^{-3}$ kg/(sec·m), and as the disperse phase, water droplets with $\rho_{20}^0 = 1000$ kg/m^3. The spacing between plates in the packet of louvers was $R = 10^{-1}$ m. Figure 1 gives gas and droplet streamlines along the direction of the flow in corrugated channels with a different amplitude of the generatrix of the lateral walls of the louvers. The figure shows that an increase in $\widetilde{A}$ gives rise to zones of return circulatory gas flow, these zones being larger the more distant they are from the inlet cross section. Apart from reducing the droplet separation on the channel walls, these zones increase the drag of a cleaning unit. Calculations indicate that, for a specified degree of cleaning, the drag is minimum for louvers with $\widetilde{A}/R \cong 1/2$. Figure 2 presents gas and droplet streamlines for various values of the mass content of water droplets at the channel inlet m_{20} and their diameter d. Calculations showed that in all flow modes the droplet streamlines for $d \geq 80\ \mu$m are virtually identical. As d decreases the flow pattern begins to change. At large m_{20} ($m_{20} > 1$), starting with $d = 20\ \mu$m and less the droplets residing at the channel center do not deposit on the louver walls but instead are carried out of them by the gas flow. With decreasing m_{20} the deposition coefficient of the droplets increases for $d = 20\ \mu$m, and when $m_{20} \leq 0.1$, all droplets of this diameter deposit on the lateral walls of the channel. A further decrease in d causes the flow structure to change at large m_{20}. Thus, for example, at $m_{20} = 1$ and $d = 10\ \mu$m, due to the intensity of interphase interaction the flow is rectified, and zones of return circulatory gas flow form in bottom regions of the channel, these zones being larger the more distant they are from the inlet cross section of the channel. Figure 2 shows that at any values of m_{20} droplets with $d \leq 10\ \mu$m practically do not deposit on the channel walls, which is in line with experimental data [7].

Figure 3 plots the efficiency of the louvers η vs the Stokes number. The figure shows that at a low moisture content ($m_{20} \leq 5\%$) it is possible to obtain a high degree of cleaning ($\eta \cong 97\%$) for louvers with $\widetilde{A}/R \cong 0.5$. A rise in m_{20} sharply decreases η, which necessitates an increase in $\widetilde{A}/R$, and this complicates the flow structure significantly, icreases the drag of the louvers, and noticeably hinders numerical realization of system of equations (1). Obviously, in this case in the Eulerian step of the method of large particles it is necessary to employ a

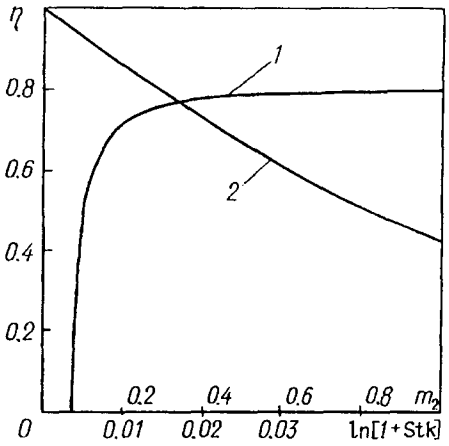

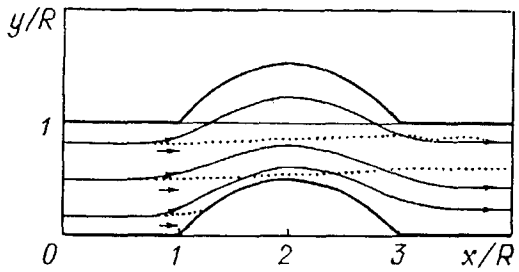

Fig. 3. Cleaning efficiency for a gas-droplet flow in louvers: 1) $m_{20} = 1$, 2) Stk = 0.005 ($d = 80\ \mu$m).

Fig. 4. Gas and droplet streamlines for a circular segment with an internal disperse flow ($M_0 = 0.08$, Stk = 6.4, $m_{20} = 0.001$).

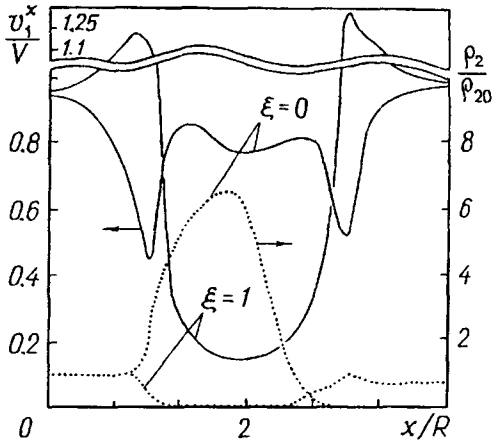

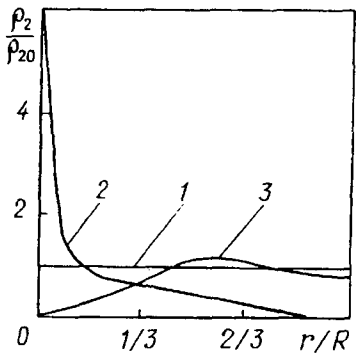

Fig. 5. Distribution of the gas velocities and the mass concentrations of droplets along the bottom ($\xi = 0$) and top ($\xi = 1$) surfaces of the channel.

Fig. 6. Distribution of the concentration of droplets in various cross sections of a channel: 1) $x/R = 1$, 2) 2, 3) 3.

time-implicit numerical scheme for calculating not only the pressure field but also the velocity fields of the carrier phase.

Figure 4 shows streamlines of the carrier phase and the droplets in an axisymmetric channel with the generatrices of its lateral surface consisting of two parallel straight lines and circular arcs. At the channel inlet ($x = 0$) $v_1^y = v_2^y = 0$. It is clear from the figure that, for the given Stk number, droplets whose radius of admission in the initial cross section varied from 0 to 1/2 completely fall on the lower circular arc of the lateral surface of the channel. Figure 5 indicates that the distribution of v_1^* along the line $\xi = 0$ has a profile that is characteristic of that observed for a sphere in a "pure" (without particles) gas. Ahead of and behind the sphere, v_1^x has the minimum value, and on its rear part, the maximum. On the line $\xi = 1$ at the points of flow turn ($x/R = 1.3$) v_1^x attains a maximum, and in the bottom region ($x/R = 2$), a minimum. Analysis of the density distribution of droplets reveals that the concentration is maximum on the rear part of the circular arc of the line $\xi = 0$ in the vicinity of the point $x/R = 2$. It can also be noted that the droplets practically do not separate out on the bottom part of the upper circular arc. Figure 6 shows the concentration distribution of the droplets in various channel cross sections. It is of interest to note that in the cross section $x/R = 3$ it has a nonmonotonic character. This is associated with the fact that with a flow over the lower circular arc, due to interaction with the gas the vertical velocity component v_2^y

increases markedly for droplets whose radius of escape from the initial cross section is larger than 0.5, which causes the droplet streamlines in the cross section $x/R = 3$ to converge.

The computational runs conducted for various configurations of channels and tubes revealed that the expounded modification of the difference scheme of the method of large particles allows numerical modeling of multiphase flows over a wide range of governing parameters. Here, as test calculations indicate, fairly high accuracy of the results (of the order of 1–3%) is attained.

NOTATION

x, spatial coordinate; t, time; R, channel width; $\tilde{A}$, amplitude of the generatrix of the louvers; L, channel length; d, droplet diameter; m, mass concentration of droplets; ρ, density; p, gas pressure; T, temperature; E, total energy; e, internal energy; $\vec{v}$, velocity vector; v^x and v^y, velocity components along the coordinate axes; u and v, velocity components of the gas in the Eulerian step; γ, adiabatic exponent of the gas; c_2 and c_{v1}, specific heat of the droplets and the gas (at constant volume); λ, thermal conductivity; μ, dynamic viscosity; Σ, surface tension; M, Mach number; Stk, Stokes number; We, Weber number; Re_{12}, Reynolds number of the relative flow over a droplet; A, B, and C, matrices of the coefficients of the approximation viscosity; Δ_f, terms not containing second derivatives of the variable f; Δt, temporal integration step; Δx, spatial integration step. Superscripts and subscripts: k, summation over the coordinate axes; s, phase number; n, number of the time layer; i and j, centers of cells of the calculation region; 0, value of the parameter in the undisturbed flow.

REFERENCES

1. R. I. Nigmatulin, Dynamics of Multiphase Media, Vol. 1 [in Russian], Moscow (1987).
2. A. G. Ageev, V. B. Karasev, I. G. Serov, and V. F. Titov, Separators of Nuclear Electric Power Plants [in Russian], Moscow (1982).
3. I. M. Vasenin, V. A. Arkhipov, V. G. Butov, et al., Gasdynamics of Two-Phase Flows in Nozzles [in Russian], Tomsk, 1986.
4. D. Anderson, G. Tannehill, and R. Pletcher, Computational Hydromechanics and Heat Transfer, Vol. 1 [Russian translation], Moscow (1990).
5. O. M. Belotserkovskii and Yu. M. Davydov, Method of Large Particles in Gasdynamics [in Russian], Moscow (1982).
6. I. Kh. Enikeev, O. F. Kuznetsova, V. A. Polyanskii, and E. F. Shurgal'skii, Zh. Vych. Mat. Mat. Fiz., 28, No. 1, 90-100 (1988).
7. V. N. Uzhov, A. Yu. Val'dberg, B. I. Myagkov, and I. K. Reshidov, Cleaning of Industrial Gases of Dust [in Russian], Moscow (1984).